Structure of the Jab1/MPN Domain and Its Implications for Proteasome Function†

Huong J. T. T. Tran,‡ Mark D. Allen,‡ Jan Löwe,§ and Mark Bycroft*,‡

MRC Centre for Protein Engineering and MRC Laboratory of Molecular Biology, Hills Road, Cambridge CB2 2QH, U.K.

Received June 16, 2003; Revised Manuscript Received August 5, 2003

ABSTRACT: The 26S proteasome is responsible for the degradation of polyubiquitinated proteins. During this process the polyubiquitin chain is removed. The identity of the proteasomal component that is responsible for this activity has not been clear, as it contains no subunits that resemble known deubiquitinating enzymes. The Jab1/MPN domain is a widespread 120 amino acid protein module found in archaea, bacteria, and eukaryotes. In eukaryotes the Jab1/MPN domain is found in subunits of several multiprotein complexes including the proteasome. Recently it has been proposed that the Jab1/MPN domain of the proteasomal subunit Rpn11 is responsible for the removal of the polyubiquitin chain from substrate proteins. Here we report the crystal structure and characterization of AF2198, a Jab1/MPN domain protein from *Archaeoglobolus fulgidus*. The structure reveals a fold that resembles that of cytidine deaminase and places the Jab1/MPN domain in a superfamily of metal dependent hydrolases.

The controlled degradation of proteins via the ubiquitin-proteasome pathway plays a major role in a variety of cellular processes including cell cycle control, DNA repair, antigen presentation, vesicle transport, the regulation of signal transduction pathways, and transcription (*1*). Proteins are targeted for degradation by the attachment of a polyubiquitin chain to a lysine residue. Degradation of polyubiquitin-tagged proteins is carried out by a multisubunit protease, the 26S proteasome (*2*). During this process the isopeptide bond between the C-terminus of ubiquitin and a lysine residue of the targeted protein is cleaved and the ubiquitin chain is released (*3*). The proteasome contains no subunits that resemble known deubiquitinating enzymes, and the identity of the component that mediates ubiquitin chain release has not been clear. Recently it has been suggested that the deubiquitination is carried out by the Rpn11 subunit of the 19S proteasome lid (*4*−*6*). Rpn11 contains a Jab1/MPN[1] (Mpr1, Pad1 N-terminal) domain, a protein module found in bacteria, archaea, and eukaryotes (*7, 8*). Rpn11, like many Jab1/MPN domain containing proteins, contains the sequence $EX_nHXHX_{10}D$ where X is any residue. Mutation of the conserved histidine and aspartate residues of this so-called JAMM (Jab1/MPN domain metalloenzyme) motif has been shown to be lethal in yeast and lead to proteolytic defects *in vivo* and the accumulation of polyubiquitinated substrates. The pattern of conserved residues in the JAMM motif is similar to those that form zinc binding sites in enzymes, and deubiquitination is inhibited when the 19S complex is incubated with a zinc chelator. The JAMM motif is also present in the Jab1/Csn5 subunit of the COP9 signalosome, a multiprotein complex with a subunit composition similar to that of the proteasome lid that cleaves the ubiquitin-like protein, Nedd8, from SCF ubiquitin ligase (*9*). This activity is also compromised by mutations of the JAMM motif and the addition of a zinc chelator (*10*). Although these data strongly suggest that in these proteins the JAMM motif corresponds to the active site residues of a metalloisopeptidase, it has not been possible to obtain direct biochemical evidence for this, as it has proved difficult to isolate individual subunits of these large multiprotein complexes in an active form. In eubacteria and archaea, the Jab1/MPN domain is usually found in single domain proteins that should be more amenable to study (*5*). To learn more about this domain, we have determined the structure of AF2198, a protein containing a JAMM motif from the archaea *Archaeoglobus fulgidus*.

MATERIALS AND METHODS

Bacterial Expression and Protein Purification. A polymerase chain reaction (PCR) was used to amplify the gene encoding AF2198 protein from *Archaeoglobus fulgidus* DNA and clone it into a pRSETA vector (Invitrogen) that has been modified to enable protein to be expressed with a thrombin cleavable N-terminal hexa-histidine tag. The plasmid was transformed into C41 (DE3) cells (*11*). Cells were grown at 37 °C until the OD_{600} reaches 0.8 and were induced with 1 mM IPTG and grown for 6 h. Cells were lysed by sonication and purified on a 25 mL Ni−NTA Superflow affinity column (Qiagen), followed by thrombin cleavage for 72 h at 37 °C to yield AF2198. Cation-exchange chromatography was used for further purification. A final gel filtration step used a Superdex 75 HR column (Amersham Pharmacia) equilibrated in 50 mM potassium phosphate buffer pH 8.0, 100 mM NaCl.

† This work was supported by a grant from Medical Research Council.

* To whom correspondence should be addressed. E-mail: mb10031@cus.cam.ac.uk.

‡ MRC Centre for Protein Engineering.

§ MRC Laboratory of Molecular Biology.

[1] Abbreviations: Af, *Archaeoglobolus fulgidus*; Jab1/MPN, Mpr1, Pad1 N-terminal; JAMM, Jab1/MPN domain metalloenzyme; AF2198, *Archaeoglobolus fulgidus* hypothetical protein.

10.1021/bi035033g CCC: $25.00
Published on Web 09/11/2003

Each mutant was made by designing two oligonucleotides, one overlapping the area to be mutated and containing the intended base(s) change and the other complementary to the first. PCR was performed using *PfuTurbo* DNA polymerase that generated a whole plasmid. *DpnI* was added into the PCR products and incubated at 37 °C for 1 h to digest the unmethylated, nonmutated parental DNA template. The DNA was transformed into XL1 supercompetent cells (Stratagene) for plasmid extraction followed by transformation into C41 cells. Cells were grown and proteins were purified as above.

Circular Dichroism Measurement. All circular dichroism measurements were carried out in the presence of 100 mM NaCl, 50 mM potassium phosphate, pH 7.0, and 1 mM DTT at 25 °C and at the wavelength 222 nm. The experiments were measured by using an Aviv 202SF spectropolarimeter (Aviv Associates, Lakewood, NJ) with the protein sample concentration 5 μM (0.6 mL), in the same buffer.

Crystallization and Data Collection. The purified protein was concentrated to 40 mg mL^{-1} in buffer containing 2 mM DTT and 10 mM Tris-HCl, pH 7.0, and crystallized in sitting-drop vapor diffusion against a reservoir containing 11% PEG 4000, 100 mM $MgCl_2$, 100 mM Tris-HCl, pH 7.8. Crystals grew in the $P2_1$ space group (grown at 17 °C, cell dimensions for the native $a = 38.22$, $b = 87.23$, $c = 67.45$ Å, $\beta = 93.97$ Å) with four molecules in the asymmetric unit. Heavy atom derivatives were prepared by soaking the crystals in the heavy atom reagents at the concentrations 5−10 mM for about 12 h. Data sets for native ($MgCl_2$), platinum (K_2PtCl_4), and mercury (EMTS) derivatives were collected in-house using a MAR-345 imaging-plate detector (MAR-Research, Hamburg, Germany) mounted on a Rigaku RUH3R generator to 1.7, 2.0, and 2.0 Å, respectively. The data set of the zinc form ($ZnCl_2$) was collected at the European Synchrotron Radiation Facility (ESRF) on beam line ID14-4 to 1.5 Å. The native data set has an $R_{merge} = 3.4\%$ (last shell, 13.0%) with overall completeness 96.5% (84.5%), and $R_{merge}(ZnCl_2) = 6.7\%$ (last shell, 33.8%) with overall completeness 85.6% (78.6%). All data were indexed and integrated using the Mosflm package (*12*) and further processed using the CCP4 suite (*13*) programs.

Structure Determination and Refinement. The crystal structure of the protein was solved using multiple isomorphous replacement with anomalous scattering (MIRAS). Phases were obtained using heavy atom derivatives and anomalous dispersion and were calculated using Solve (*14*). Resolve (*15*) was used for solvent flattening, assuming a 50% solvent content with the magnesium form as the native set. Model building and refinement was carried out using the programs MAIN (*16*) and CNS (*17*), respectively. During the final stages of refinement 278 water molecules, four zinc ions, and two Tris molecules were added. The presence of the zinc ions was confirmed by calculating anomalous difference electron density maps. The zinc structure was refined to 1.5 Å and has 92.8% of the residues in the maximum allowed region and three in the disallowed region of the Ramachandran map. The final structure of AF2198 has an *R*-free value of 24.2%, an *R*-work value of 21.3%, and an average temperature factor of 24.98 Å^2. The model has an rms deviation from ideal values in bond length of 0.006 Å and in bond angle of 1.395°. Figures were prepared using Molscript (*18*).

Table 1: Data Statistics

Data Collection				
data set	native	$ZnCl_2$	K_2PtCl_4	EMTS
wavelength	1.5418 Å	0.9790 Å	1.5418 Å	1.5418 Å
space group	$P2_1$	$P2_1$	$P2_1$	$P2_1$
$a =$	38.22 Å	37.64 Å	38.27 Å	38.20 Å
$b =$	87.23 Å	87.46 Å	87.57 Å	87.22 Å
$c =$	67.45 Å	67.87 Å	67.56 Å	67.38 Å
$\beta =$	93.97 Å	93.92 Å	94.08 Å	93.88 Å
resolution range (Å)	14.6−1.7	25.0−1.5	14.4−2.0	14.8−2.0
unique reflections	46,882	69,516	30,082	29,030
completeness (%) overall (final shell)	96.5 (84.5)	85.6 (78.6)	99.2 (96.3)	97.4 (95.6)
R_{merge}[a] (final shell)	0.034 (0.130)	0.067 (0.338)	0.056 (0.212)	0.050 (0.191)

Refinement	
R-factor[b] (R_{free})	21.3 (24.2)
resolution range (Å)	50−1.5
rms deviation from ideality	
bonds (Å)	0.006
angles (deg)	1.395
avg *B*-factors (Å)^2	24.98

[a] $R_{merge} = \sum_{hkl}\sum_i |I(I)I/\sum_{hkl}\sum_i(I)$. [b] $R\text{-factor}_r = \sum_{hkl}||F_{obs}| - k|F_{calc}|/\sum_{hkl}||F_{obs}|$.

RESULTS AND DISCUSSION

Overall Structure. AF2198 was expressed in *E. coli*, purified and crystallized. The structure of AF2198 was determined to 1.5 Å resolution using multiple isomorphous replacement with anomalous scattering (Table 1). Crystals of AF2198 contain four molecules in the asymmetric unit arranged as two dimers. In solution, AF2198 behaves as a monomer upon the basis of its migration on a Superdex-75 analytical gel filtration column (data not shown). Crystal contacts between the two molecules in each dimer involve active site residues, which could mimic protein−substrate interactions. As the four molecules are structurally identical, the remainder of the discussion will focus solely upon monomer A. AF2198 is a compact, single domain protein (Figure 1b). It is composed of a five-stranded mixed β-sheet with strand order 21345 sandwiched between two α-helices. There is a second smaller three-stranded parallel β-sheet formed by residues at the N and C termini and in the loop between the first two strands of the main sheet. Jab1/MPN domains often form part of larger proteins. The N and C termini of the structure are close in space, allowing it to be easily inserted into a multidomain protein. A structure-based alignment of representative Jab1/MPN domains is shown in Figure 2. Hydrophobic core residues are conserved; insertions and deletions are restricted to loops between elements of secondary structure. It is therefore likely that the majority of Jab1/MPN domains have a structure very similar to that of AF2198.

JAMM Motif. The histidine and aspartate residues of the JAMM motif coordinate a zinc ion (Figure 3). The histidine residues (His 70 and His 72) are in the third strand of the main β-sheet. The aspartate residue (Asp 83) is in the second α-helix. The glutamate residue of the JAMM motif (Glu 25) is in the loop between the first helix and the second strand of the sheet. Many Jab1/MPN domains contain a serine residue two residues before the aspartate of the JAMM motif. In AF2198, this residue (Ser 80) is situated in the loop between the third strand of the main sheet and the second helix. All of the conserved residues cluster together at the end of a cleft in the protein surface in an arrangement that

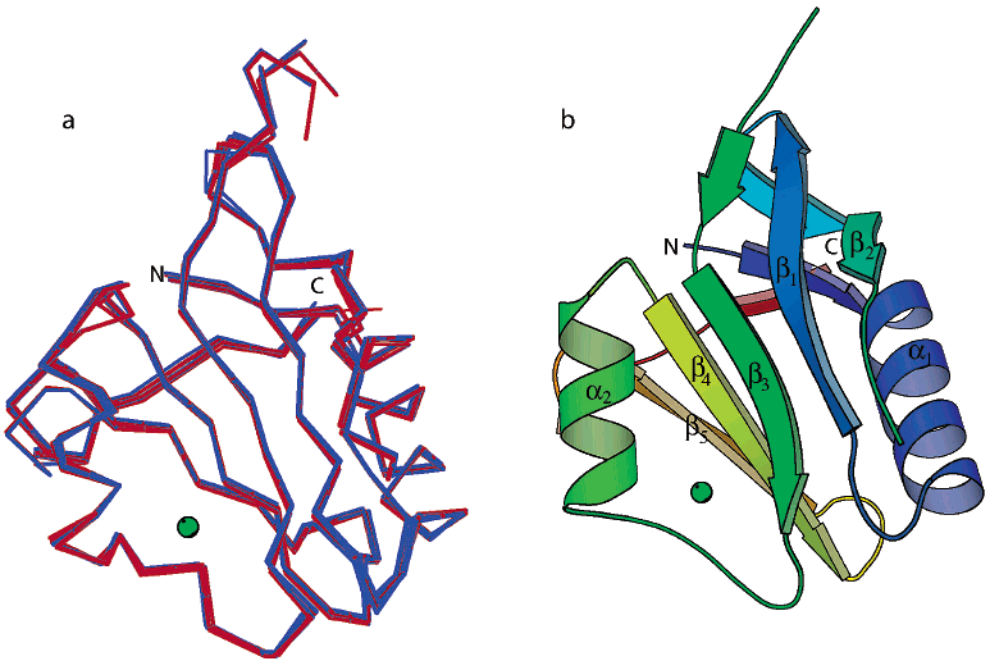

FIGURE 1: (a) Superposition of the backbone of four molecules in the asymmetric unit of the zinc-free form (blue) and four molecules in the asymmetric unit of the zinc form (red). (b) Overall structure of AF2198 (PDB ID code 1oi0) shown in cartoon representation. The molecule is colored from the N-terminus to the C-terminus such that the colors follow the colors in the visible spectrum (blue at the N-terminus). The zinc ions are shown as green spheres. The N- and C-termini are labeled.

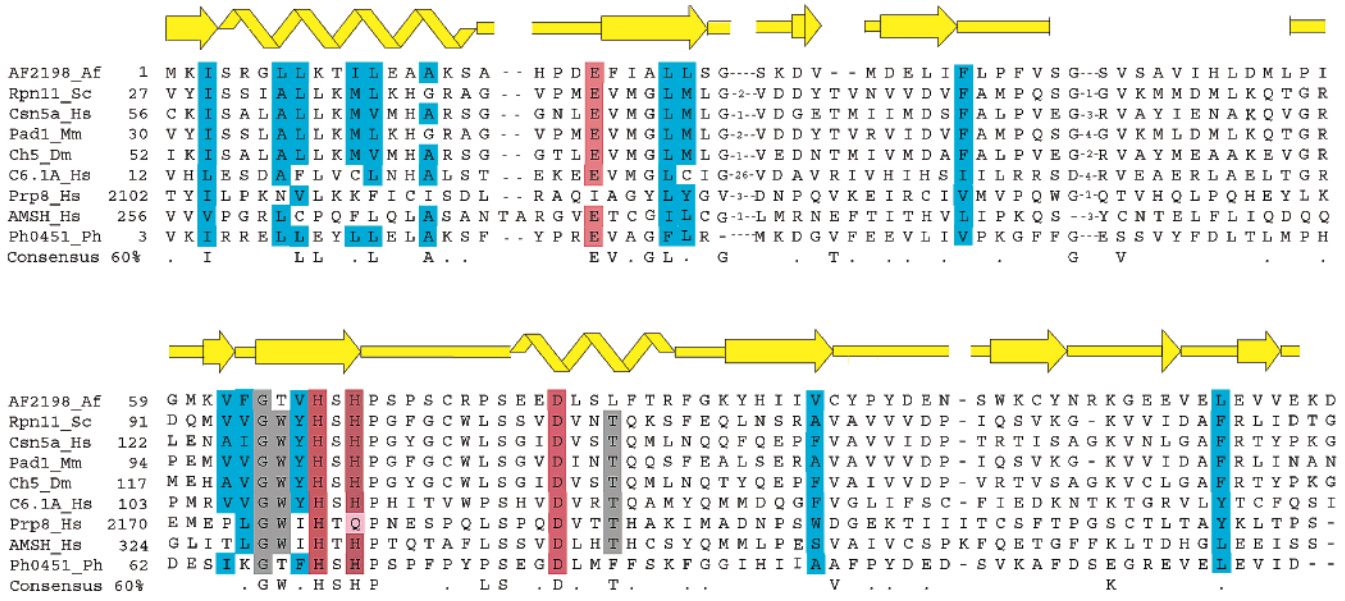

FIGURE 2: Alignment of representative MPN domain proteins. Selected sequences were aligned using Clustal W and modified manually to ensure correct superposition of the conserved motif. Residues that are conserved in the JAMM motif are colored red; residues that are conserved in the groove and may potentially be involved in substrate interaction are colored gray. The conserved hydrophobic core residues are highlighted in blue. Secondary structures found in the structure are indicated above the sequence alignments. GI numbers are as follows: *Archaeoglobulus fulgidus* AF2198, 2648331; *Saccharomyces cerrvisiae* Rpn11, 1171012; *Homo sapiens* Csn5a, 12654695; *Mus muslucus* Pad1, 2505940; *Drosophila melanogaster* Ch5, 7300154; *Homo sapiens* C6.1A, 20532383; *Homo sapiens* Prp8, 17999536; *Homo sapiens* AMSH, 17738303; *Pyrococcus horikoshii* Ph0451, 14590365.

is consistent with an enzyme active site (Figure 3). Mutation of the histidine and aspartate residues of the JAMM motifs of Jab1/Csn5 and Rpn11 has been shown to block the deneddylation and deubiquitinating activity of the signalosome and proteasome. These results have been taken to indicate that the JAMM motif forms part of the active site of an isopeptidase in these proteins. One caveat to this conclusion is that it was not known if these mutations disrupted the structure of the proteins. The equivalent residues in the AF2198 structure are all solvent exposed, and their substitution with alanine has no substantial effect on the circular dichroism spectrum or stability of the protein (data not shown). In addition, the removal of the zinc ion in AF2198 produces only a minor rearrangement of the residues in the active site cleft (Figure 4), and the backbones of zinc-free and zinc forms are superimposable (Figure 1a). On the basis of these findings, it can be concluded that the mutations of residues in the JAMM motifs of Jab1/Csn5 and Rpn11

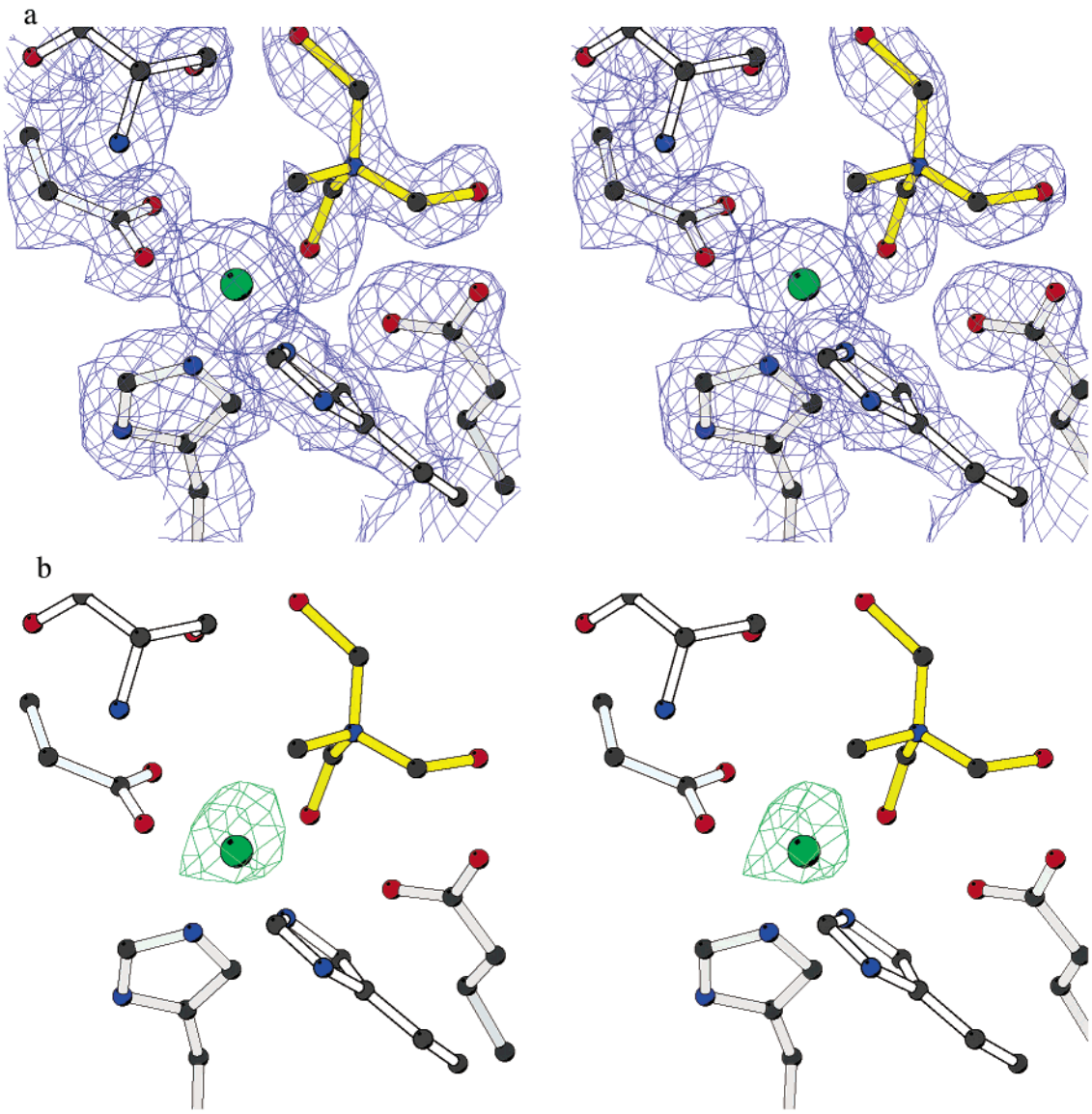

FIGURE 3: Stereoview of the active site with the electron density map, showing the anomalous difference Fourier synthesis at a wavelength of 0.9790 Å: (a) contour level at 1σ; (b) contour level at 6σ. The coordinated zinc ions are shown as green spheres. Clockwise: Tris (yellow), Glu25, His72, His70, Asp83, and Ser80.

have no significant structural consequences and that the effects of these substitutions are a direct result of the elimination of catalytically important residues.

Homology to Cytidine Deaminase. Comparison of the structure of AF2198 with other protein structures using the DALI server (*19*) reveals similarity (Dali Z score 4.7) to cytidine deaminase (Figure 5), a zinc metalloenzyme that catalyzes the hydrolytic deamination of cytidine to uridine (*20*, *21*). Despite the absence of significant sequence similarity, the structures are superimposable over 46 residues in the central sheet and two of the helices with the C_α root-mean-square (rms) deviation of 2.0 Å. This degree of structural similarity is sufficient to conclude that these proteins are evolutionarily related and places the Jab1/MPN domain in a superfamily of metal dependent hydrolases. The catalytic mechanism of cytidine deaminase has been studied in detail (*22*). The zinc ion activates a water molecule to form a hydroxide ion that in turn makes a nucleophilic attack on the C4 carbon in the pyrimidine ring of cytidine, resulting in the formation of a tetrahedral intermediate. This then collapses, eliminating ammonia, leading to the replacement of the amino group of cytidine with an oxo group stemming from the water initially coordinated to the zinc ion. It is likely that the zinc ion in the Jab1/MPN domain of Rpn11 performs a similar role during isopeptide bond hydrolysis. Cytidine deaminase contains a highly conserved glutamate residue that is positioned near to the active site zinc. This residue functions both as a proton acceptor and donor during the deamination reaction, and the glutamate residue of the JAMM motif probably plays a similar role.

The positions of two of the zinc ligands differ in cytidine deaminase, as it has an extra helix that packs across the sheet that contains the histidine residues of the JAMM motif in AF2198. In cytidine, deaminase residues in this additional helix and in the turn that precedes the helix that contains the conserved zinc ligand coordinate the metal ion (Figure 5). The structures of several cytidine deaminases have been determined, and all of them have this type of zinc coordination. The absence of the helix in AF2198 produces a hydrophobic groove on the protein's surface close to the catalytic zinc ion that could potentially be involved in substrate binding. In the crystal lattice many of the inter-

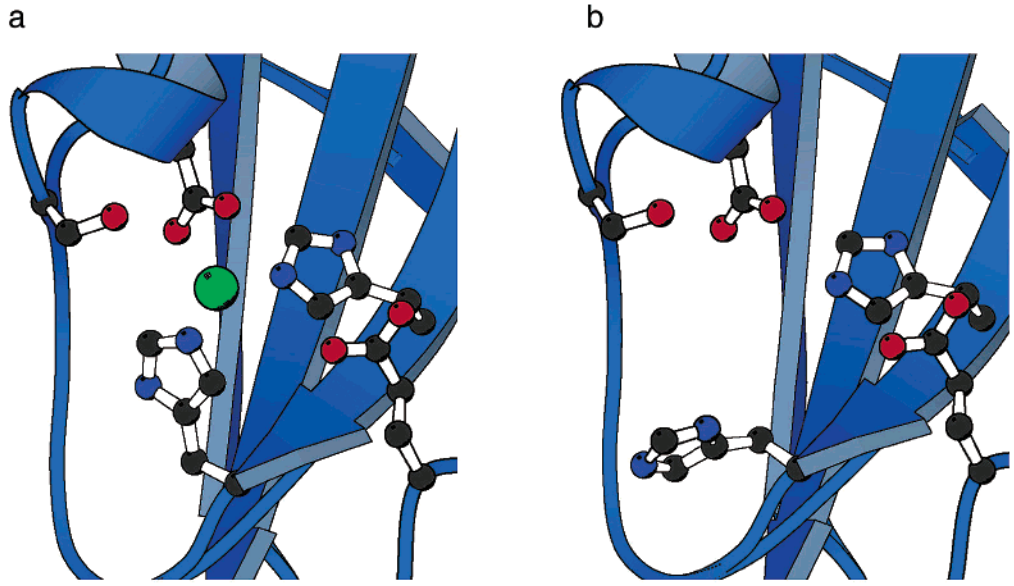

FIGURE 4: Active site of AF2198 in the (a) zinc form and in the (b) zinc-free form showing a minor rearrangement of the His residue.

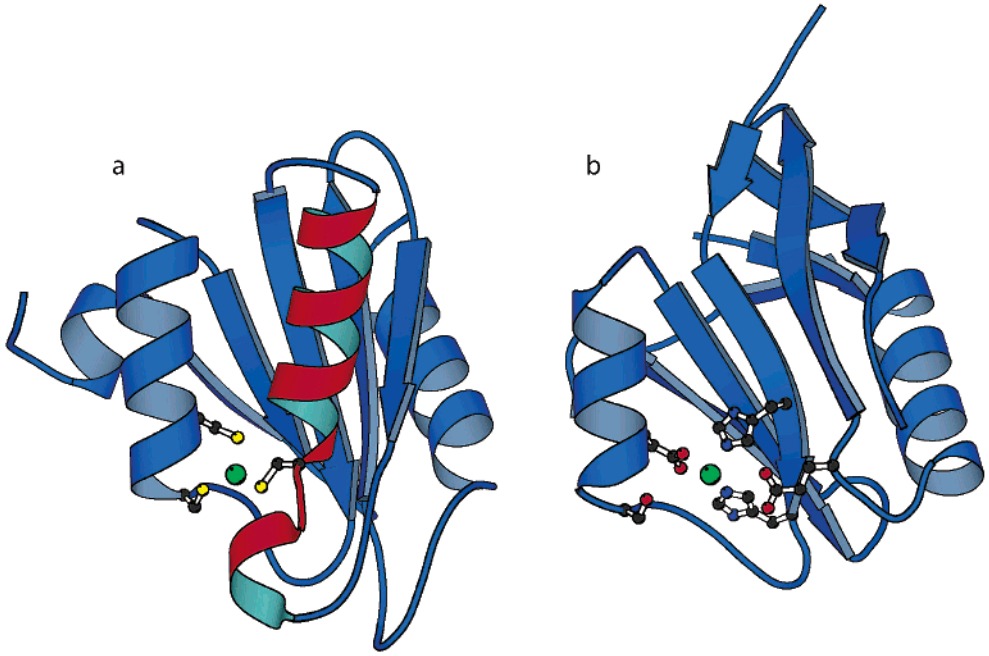

FIGURE 5: Comparison of the structure of (a) one subunit of the tetramer cytidine deaminase (PDB ID code 1jtk) and (b) AF2198. The residues that coordinate zinc in both proteins are represented as balls-and-sticks. The zinc ions are shown as green spheres. The additional α-helix in the deaminase is colored red.

molecular contacts involve residues in this groove, and these probably mimic protein substrate interactions. Interestingly, in Rpn11, Jab1/Csn5, and a number of other eukaryotic proteins, there are several conserved residues in this region that could be involved in recognizing protein substrates.

Sequence Variation in Jab1/MPN Domains. In bacteria and archaea most Jab1/MPN domains are found in proteins that consist of an isolated domain, the majority of which have a JAMM motif. These fall into distinct families with characteristic patterns of sequence conservation. Jab1/MPN domains containing the JAMM motif are also present in bacterial RadC DNA repair proteins, in phage and prophage proteins involved in tail assembly, and in a family of bacterial proteins in which they are fused to NlpC/p60 cell-wall peptidase domains (*23*).

As well as being present in subunits of the proteasome and signalosome, the Jab1/MPN domain is also found in a number of other human proteins. Many of these have a JAMM motif. These include AMSH (associated molecule with the SH3 domain of STAM), proteins involved in transcriptional regulation, and C6.1A, a protein that is fused to the T-cell receptor in pro-lymphocytic T-cell leukemia. It is possible that these proteins also have isopeptidase activity and are involved in the regulation of ubiquitin and ubiquitin-like protein conjugation. In the Jab1/MPN domain of the splicing factor Prp8, one of the histidine residues of the JAMM motif is replaced by a glutamine (Figure 2). It is possible that the JAMM motif of this protein is still active, and if so, it could provide a link between RNA splicing and the ubiquitin pathway. In a subset of Jab1/MPN domains,

one or more of the zinc binding residues are replaced by amino acids that cannot ligate zinc. These include components of the eukaryotic initiation factor 3 complex and the Rpn8 subunit of the proteasome lid. As the structures of the zinc bound and zinc free forms of AF2198 are very similar, it is likely that these proteins have a similar fold to that of Jab1/MPN domains that contain a JAMM motif. They are, however, probably not catalytically active.

Biochemical, mutagenesis, and now structural data all suggest that within the proteasome and signalosome Jab1/MPN domains hydrolyze isopeptide bonds between the C-terminus of ubiquitin or ubiquitin-like proteins and lysine side chains. Protein conjugation via isopeptide bond formation is however only known in eukaryotes. The role of the Jab1/MPN domain in bacteria and archaea is therefore not clear. These organisms do contain the ubiquitin homologues MoaD and ThiS. These proteins form thioester bonds to the E1-like enzymes MoeB and ThiF in molybdopterin and thiamine biosynthesis, respectively (*24*). There is, however, no isopeptide bond formation in these pathways.

The most widespread family of deubiquitinating enzymes are related to cysteine proteases (*25*). It is possible that Jab1/MPN domains may also be proteases that in the setting of the proteasome have evolved to cleave isopeptide bonds. The Jab1/MPN domain structure however differs from those of other known zinc proteases. It also lacks features typically seen in proteases such as an obvious peptide-binding site. We could not detect any protease activity for AF2198 using a variety of protein substrates. It is possible that, rather than acting as proteases, other Jab1/MPN domains function as hydrolases that remove modifications from the ends of lysine side chains. As lysine modifications such as acetylation are widespread in all forms of life, this function is consistent with the distribution of the domain.

CONCLUSIONS

The structural data presented here, taken together with previously reported biochemical and genetic results, firmly establish Rpn11 as the component of the proteasome that is responsible for the deubiquitination of protein substrates. Inhibitors of the proteasome show promise as therapeutic agents (*26*). To date these have been targeted at the central proteolytic chamber. Deubiquitination is essential for proteasomal function, as the ubiquitin chains have to be removed to allow the targeted protein to enter the central cavity. This stage of the cycle is therefore also a candidate for inhibition. As many successful drugs bind to zinc containing enzymes, the inhibition of the Jab1/MPN domain of Rpn11 offers an attractive target. The structure reported there can be used as a basis for these efforts.

ACKNOWLEDGMENT

We thank Alexey Murzin for advice and comments and Roger Williams and Olga Perisic for advice on heavy atom derivatives.

REFERENCES

1. Hershko, A., and Ciechanover, A. (1998) *Annu. Rev. Biochem. 67*, 425−79.
2. Voges, D., Zwickl, P., and Baumeister, W. (1999) *Annu. Rev. Biochem. 68*, 1015−68.
3. Eytan, E., Armon, T., Heller, H., Beck, S., and Hershko, A. (1993) *J. Biol. Chem. 268*, 4668−74.
4. Verma, R., Aravind, L., Oania, R., McDonald, W. H., Yates, J. R., 3rd, Koonin, E. V., and Deshaies, R. J. (2002) *Science 298*, 611−5.
5. Maytal-Kivity, V., Reis, N., Hofmann, K., and Glickman, M. H. (2002) *BMC Biochem. 3*, 28.
6. Yao, T., and Cohen, R. E. (2002) *Nature 419*, 403−7.
7. Aravind, L., and Ponting, C. P. (1998) *Protein Sci. 7*, 1250−4.
8. Hofmann, K., and Bucher, P. (1998) *Trends Biochem. Sci. 23*, 204−5.
9. Lyapina, S., Cope, G., Shevchenko, A., Serino, G., Tsuge, T., Zhou, C., Wolf, D. A., Wei, N., and Deshaies, R. J. (2001) *Science 292*, 1382−5.
10. Cope, G. A., Suh, G. S., Aravind, L., Schwarz, S. E., Zipursky, S. L., Koonin, E. V., and Deshaies, R. J. (2002) *Science 298*, 608−11.
11. Miroux, B., and Walker, J. E. (1996) *J. Mol. Biol. 260*, 289−98.
12. Leslie, A. (1991) in *CCP4 and ESF-EACMB Newsletters on Protein Crystallography*, SERC Laboratory, Daresbury, Warrington, U.K.
13. Collaborative Computational Project, N. (1994) *Acta Crystallogr. D50*, 760−763.
14. Terwilliger, T. C., and Berendzen, J. (1999) *Acta Crystallogr. D: Biol. Crystallogr. 55 (Pt 4)*, 849−61.
15. Terwilliger, T. C. (2000) *Acta Crystallogr. D: Biol. Crystallogr. 56 (Pt 8)*, 965−72.
16. Turk, D. (1992) Weiterentwicklung eines Programms fuer Molekuelgraphik und Elektrondichte-Manipulation und seine Anwendung auf verschiedene Protein-Strukturaufklaerungen. Ph.D. Thesis, Technische Universität München.
17. Brunger, A. T., Adams, P. D., Clore, G. M., DeLano, W. L., Gros, P., Grosse-Kunstleve, R. W., Jiang, J. S., Kuszewski, J., Nilges, M., Pannu, N. S., Read, R. J., Rice, L. M., Simonson, T., and Warren, G. L. (1998) *Acta Crystallogr. D: Biol. Crystallogr. 54 (Pt 5)*, 905−21.
18. Kraulis, P. J. (1991) *J. Appl. Crystallogr. 24*, 946−950.
19. Holm, L., and Sander, C. (1995) *Trends Biochem. Sci. 20*, 478−480.
20. Johansson, E., Mejlhede, N., Neuhard, J., and Larsen, S. (2002) *Biochemistry 41*, 2563−70.
21. Xiang, S. B., Short, S. A., Wolfenden, R., and Carter, C. W. (1995) *Biochemistry 34*, 4516−4523.
22. Snider, M. J., Lazarevic, D., and Wolfenden, R. (2002) *Biochemistry 41*, 3925−30.
23. Anantharaman, V., and Aravind, L. (2003) *Genome Biol. 4*, R11.
24. Furukawa, K., Mizushima, N., Noda, T., and Ohsumi, Y. (2000) *J. Biol. Chem. 275*, 7462−5.
25. Lo Conte, L., Brenner, S. E., Hubbard, T. J., Chothia, C., and Murzin, A. G. (2002) *Nucleic Acids Res. 30*, 264−7.
26. Adams, J. (2002) *Curr. Opin. Chem. Biol. 6*, 493−500.

BI035033G